Correlative Laser Confocal Microscopy Study and Multimodal 2D/3D Registration as Ground Truth for X-ray Inspection of Internal Defects in LPBF Manufacturing

Catherine Desrosiers[1], Morgan Letenneur[2], Fabrice Bernier[3], Farida Cheriet[1], Vladimir Brailovski[2], Nicolas Piché[4], François Guibault[1]

[1] École Polytechnique Montréal, 2500 Chemin de Polytechnique, Montréal, QC H3T 1J4, Canada, e-mail: {catherine.desrosiers, farida.cheriet, francois.guibault}@polymtl.ca

[2]École de Technologie Supérieure, 1100 Notre-Dame Ouest, Montréal, QC H3C 1K3, Canada, e-mail: morgan.letenneur.1@etsmtl.net, Vladimir.Brailovski@etsmtl.ca

[3]Centre National de Recherche du Canada, 75 de Mortagne, Boucherville, QC J4B 6Y4, Canada, e-mail: Fabrice.Bernier@cnrc-nrc.gc.ca

[4]Object Research Systems, 460 Sainte-Catherine Ouest, Suite 600, Montréal, QC H3B 1A7, Canada, e-mail: npiche@theobjects.com

Abstract

In a time when engineers working in the additive manufacturing field are interested in the standardized x-ray computed tomography (XCT) image analysis workflow, an insight into a higher resolution imaging and ground truth validation become invaluable. In this work, we propose a repeatable and automated 2D/3D registration protocol between an XCT volume and a laser confocal microscopy image, thus allowing a correlative multiscale validation and comparison study of the flaw detection capabilities and uncertainties of an XCT analysis of additively-manufactured parts. Once the spatial correlation achieved, a comparison study evaluating the level of confidence of the flaw detection and measurement computed from the XCT volume is presented. To this end, a pore-to-pore comparison between the XCT volume and the laser confocal image, which offers a 4 times higher resolution as well as a better signal to noise ratio, is carried out and various pore morphology metric distributions are compared. The generality of the proposed approach is ensured by the use of printed Ti64 LPBF samples with different levels of the intentionally seeded and controlled porosity.

Keywords: X-ray tomography, Correlative multi-scale study, Laser confocal microscopy, 2D/3D Registration, LPBF, AM

1 Introduction

It is now well established that x-ray computed tomography (XCT) represents one of the best suited technologies for the internal structure observation of 3D parts produced by additive manufacturing (AM) [1]. This image modality is indeed promising because it provides a non-destructive testing (NDT) solution which, combined with segmentation algorithms, allows the detection, the characterization and the quantification of flaws induced during the layering process of Laser Powder Bed Fusion (LPBF) manufacturing; a mandatory quality control process for a broader industrial adoption of LPBF.

Although many advancements have been completed in the field, research in AM aimed at a better understanding and standardization of the characterization by XCT is still a trending topic [2],[3]. Frequently, researchers in this area resort to higher resolution image modalities than those provided by XCT to gain insight into a corresponding region of interest (ROI) at different scales, whether for the validation of the technique proposed or for the purpose of obtaining additional information. This comparison needs spatial correlation and is often known in literature as correlative imaging [4]. In recent years, various research works have been carried out on this subject. Notably, Yang X. & al. proposed an XCT image enhancement method using information from higher resolution images and a dictionary learning approach [5]. Sundar, V & al. used an automated optical serial sectioning (AOSS), mechanical polishing and optical imaging of a sample in order to raise the XCT analysis limitations [6]. More recently, Jolley B. & al. conducted a serial sectioning study on a LPBF part to quantify and evaluate the accuracy of the state-of-the-art defect characterization methods in XCT volumes [7]. The study also aimed to propose possible improvements to the image analysis workflow. Although many multimodal registration techniques exist, Jolley and

https://doi.org/10.58286/26642

his team raised in their manuscript limitations of the automatic registration between the two modalities and suggested that this needs to be addressed in future works.

Regardless of the final outcome of the previous studies, most of them require realizing a perfect overlap between the ROIs of different image modalities. To do so, generalized and automated registration workflow is needed. In this work, we propose a reproducible 2D/3D registration protocol for a multiscale and multimodal correlative study of LPBF parts using XCT volumes (Figure 1a,b) and laser confocal microscopy (LCM) images (Figure 1c). The laser confocal microscope was selected for this study because it allows the imaging of a sample surface and the obtaining of topographical information, such as a height map of the surface [8]. Furthermore, the laser confocal microscope generates images of comparable quality to scanning electron microscopy (SEM), while taking less time and having no sample size constraints. Also, the intention here is to propose a methodology that does not require the access to an expensive AOSS system.

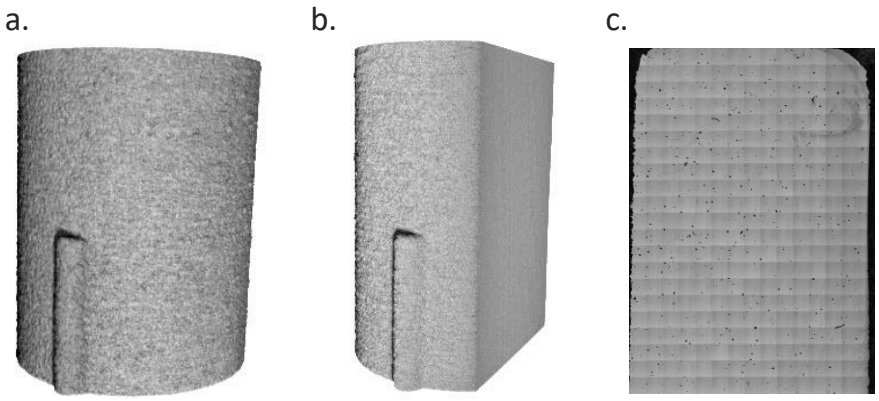

Figure 1 Registration between an XCT 3D volume and a laser confocal microscopy image: a) Full XCT volume, b) Cut XCT volume, c) Laser confocal microscope 2D image

In addition to differences in the modality and image resolution, a 2D/3D registration faces several difficulties affecting the perfect overlap between the images. Firstly, in order to proceed to microscopy imaging, the sample must be cut along a plane (Figure 1b). Performing a perfectly aligned cut with the canonical base plane represents a challenge due to a limited tool precision and could have a significant incidence on the study. With this constraint, it must be assumed that the cut surface is rather curved than plane, meaning that not all the points on the image are at the same distance from the microscope lens. Since a microscope provides a 2D planar image representation, it is then expected that distortions will be introduced by this representation, and if they are not compensated, the pores geometry and interpore distance will be inexact. Some of the difficulties of the process are also related to the fact that the features to be compared or validated are *a priori* internal to XCT volumes, meaning that the XCT imaging of a cut sample would not make the solution representative of an exact workflow of internal structure imaging. This is because the accuracy of the surface pore measurements using XCT would differ from that of the in-volume pore measurements, since the former are more affected by scattering artifacts than the latter (Figure 2a,b).

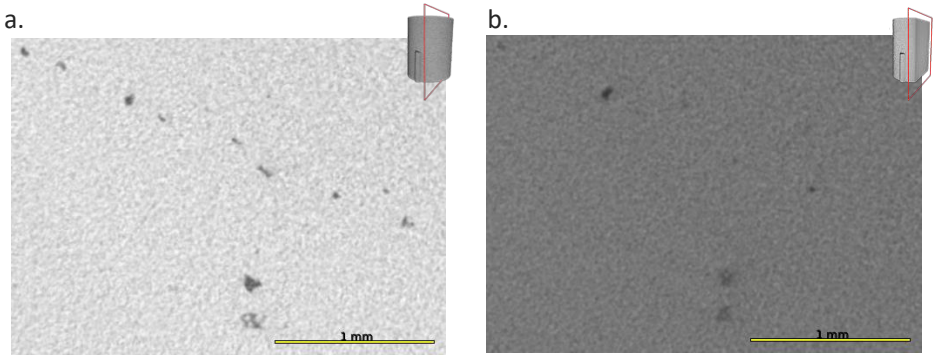

Figure 2: a) XCT pores within the full sample volume, b) XCT pores at the surface of the cut sample volume

Finally, considering the fact that a spatial fit between the surface imaged with the microscope and the XCT sample volume would not correspond to one specific XCT slice, a sub volume comprising a series of XTC slices must be used for comparison. The approach presented in this work is designed to make the solution robust to the fact that the cut plane is not voxel-aligned and represents a topography instead of a perfect plane.

2 Methods

The methodology of the proposed registration protocol for a correlative study between XCT volumes and laser confocal microscopy images can be summarized in 8 main steps presented in Figure 3. These steps correspond to the sample design and manufacturing (Figure 3a), cutting (Figure 3c) and imaging (Figure 3b, Figure 3d and Figure 3e). Then two intermediate steps, one for each imaging modality, are necessary to correct the images and inaccuracies induced by the cut and the imaging systems. First, a few slices along the normal to the cutting plane of the XCT volume are extracted (Figure 3f). Then, a 2.5D surface correction of the laser confocal microscopy image is performed (Figure 3g). These steps allow simplifying the problem for the multimodal 2D/3D registration between the laser confocal microscopy 2D image and the x-ray computed tomography volume (Figure 3h). The next section aims to further detail these steps.

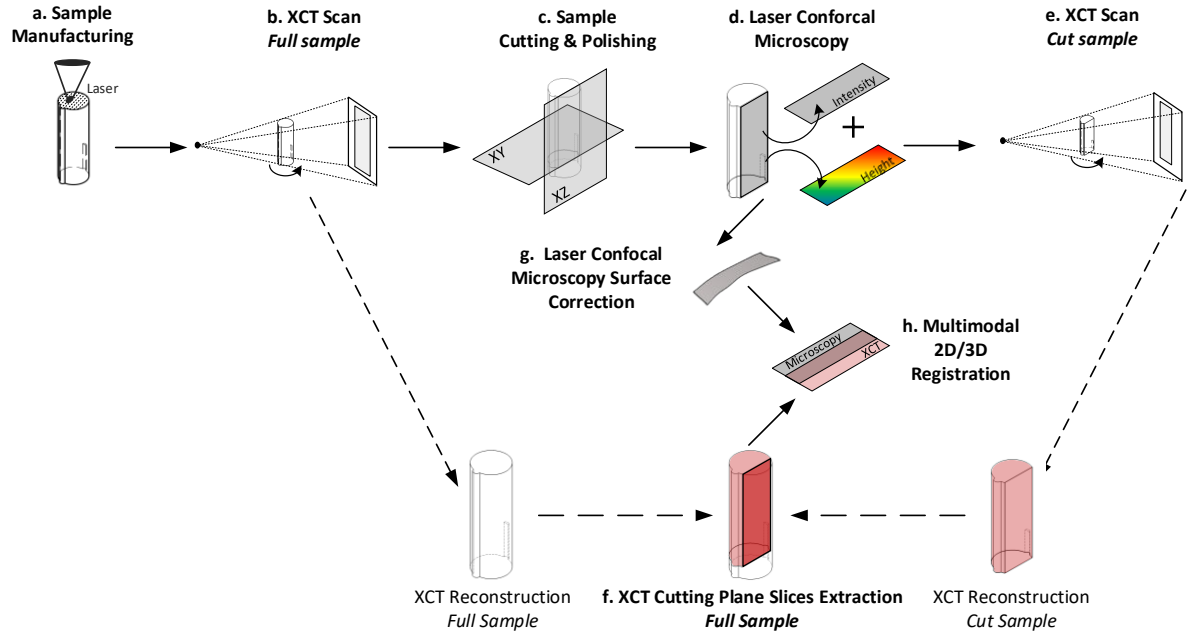

Figure 3: Overview of the 2D/3D registration protocol workflow for a multimodal and multiscale correlative study between an x-ray computed tomography (XCT) volume and a laser confocal microscopy image

Design, Manufacturing and Imaging

At first, a cylinder of 30 mm height and 10 mm diameter with two opposing longitudinally-oriented extrusions is designed (Figure 4a). The addition of these extrusions is necessary to avoid ambiguities that could arise during the subsequent image analysis because of the perfect symmetry of a standard cylindrical sample. Subsequently, three types of samples, S1, S2, S3, are manufactured from Ti-6Al-4V powder and printed with an EOSINT M280 LPBF system (EOS GmbH, Munich, Germany) equipped with a 400 W ytterbium fiber laser and a standard EOS HSS doctor blade. These samples are fabricated using three specific print parameter sets to induce in them different levels of porosity and different pore geometries and distributions [9]. In this study, two expected levels of porosity (0.3 and 0.5%), two pore geometries (spherical and elongated) and two pore distributions (random and aligned) are considered. Figure 4b and Figure 4c show, respectively, the pore geometries and distributions, while Table 1 provides the LPBF parameters used to print each sample (Figure 3a). The samples are then imaged by x-ray computed tomography (XCT) using a Nikon XTH 225 (Nikon, Brighton, MI, US) system with the acquisition parameters summarized in Table 2. Then, the 3D reconstructed volume is generated by the CT pro 3D (Nikon,

Brighton, MI, US) software. The resolution of the final XCT reconstructed volume corresponds to 8 µm (Figure 3b). Next, the samples are cut by a silicon carbide (SiC) cut-off wheel (Secotom 50, Struers, Ballerup, Danemark), immersed in epoxy resin using a LaboPress-3 (Struers, Ballerup, Danemark) system and manually polished with SiC paper up to grit 1200. Final polishing is then performed with a vibrometer and colloidal silica solution (0.05 µm grit size) (Figure 3c). They are then observed with a laser confocal LEXT4100 (Olympus, Tokyo, Japan) microscope with the MPLAPONLEXT20x lens at 1x zoom. To cover an entire cut surface, multiple images are acquired and stitched together in order to provide a final image resolution of ~2 µm, which is four times higher than that of the XCT scan images. Both data types, the height and the intensity of the laser confocal microscope acquisition are exported as CSV files (Figure 3d). Finally, the cut samples are rescanned by x-ray computed tomography, and the results obtained used as a reference for the cutting plane identification (Figure 3e). Note that only the results related to the transversal (XY plane) cut of the sample are presented in this work. The longitudinal cut will be addressed in future works.

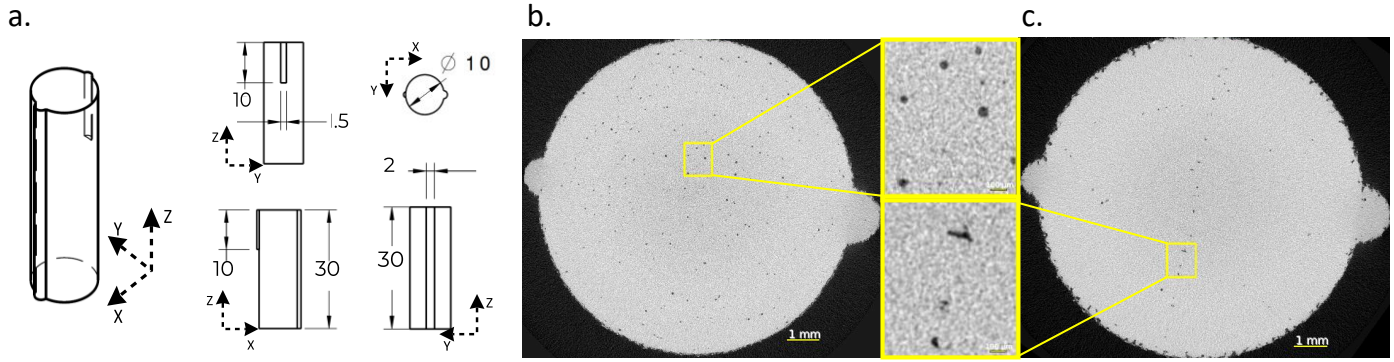

Figure 4: a) Sample design, b) spherical and random pores, c) elongated and aligned pores on the transversal (XY plane) cut of the sample

Table 1: Printing parameters, expected porosity and expected pore geometry per sample

Sample	Laser Power, W	Laser Speed, mm/s	Hatching space, µm	Layer thickness, µm	Build rate, cm^3/h	Energy density, J/mm^3	Expected porosity, %	Expected pore geometry
S1	250	757	120	60	19.6	45.8	0.5	Spherical
S2	310	920	120	60	23.8	46.8	0.3	Spherical
S3	370	1687	120	60	43.7	30.5	0.5	Elongated

Table 2 : Selected XCT Acquisitions Parameters

XCT Acquisition Parameters	**Full Sample Scan**	**Cut Sample Scan**
Voltage, kV	135	197
Current, µA	64	67
Exposure time, ms	1000	2000
Filter, mm	Copper, 0.5	Copper, 0.75
Number of frames	2634	2634
Resolution, µm	8	8

XCT Cutting Plane Slices Extraction

Knowing that the purpose of this study is to propose an approach allowing a better interpretation of the XCT images and to validate the new developed pore identification algorithms, the correlative study must use the images from the initially acquired full scan, as it would be in the context of nondestructive measurements. In order to reduce the complexity of finding an optimal solution between the microscopic image and the XCT volume, a subset of slices corresponding to the region of interest near the cutting surface is first extracted from the XCT volume. This is the reason why the second XCT acquisition of the cut sample is needed and used as a reference for the cutting plane

identification. To this end, a rigid registration between the reconstructed volume of the initial full sample and the cut sample is first processed (Figure 5a). An initial alignment is made by aligning the center of mass of both reconstructed volumes. Next, by optimizing the mutual information, an automated registration between samples is computed using the Dragonfly 2021.3 (Object Research Systems, Montreal, Qc, Canada) software [10]. Once the optimal fit is identified, an isosurface of the cut sample volume is calculated using the OTSU threshold and the marching cube algorithm [11], [12], Figure 5b. Using 3D coordinates of the vertices representing the cut surface of the isosurface mesh, the first vertex (x, y, z) coordinate allows identifying the starting image volume data location. Finally, the subset of the initial full sample XCT images is extracted from the plane identified (Figure 5c). The subset slice count is fixed to +/- 10 voxels in the normal direction. This extension of 10 voxels in each direction to the plane is done to counter the ambiguities caused by the imaging system resolutions and tools precision. A series of Python scripts and the use of Dragonfly's external developer tools (Object Research Systems, Montreal, Qc, Canada) allowed the process to be automated.

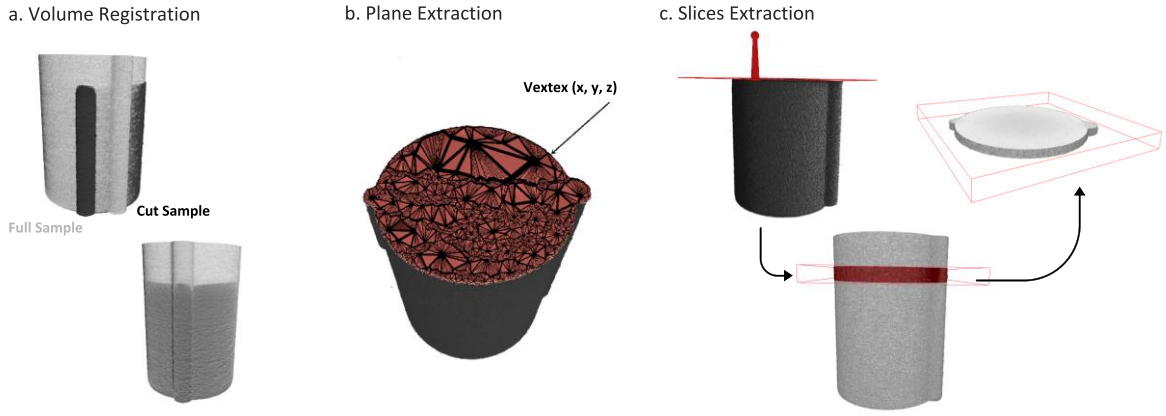

Figure 5: a) Rigid registration between the full and the cut XCT volumes, b) interpolation of the cutting plane, c) XCT slices extraction using the extended plane

Laser Confocal Microscopy Surface Correction

This step aims to correct distortions introduced in the microscopy image by the interpolation of a surface by a plane when the 2D image is acquired (Figure 6b). Note that when imaged with the laser confocal microscope, the data obtained by the laser also contains the topography representation of the sample surface through a height map between the lens and the sample (Figure 6a). This additional information allows to recover a 2.5D image and thus to correct the distortions of the microscopic image related to the interpolation, performed along the Z axis, of the surface by a plane, when the 2D image is generated by projection. To this end, a Python script is implemented to read the two previously obtained CSV files, combine the intensity and the height information and export it as a 2.5D image stack (Figure 6c).

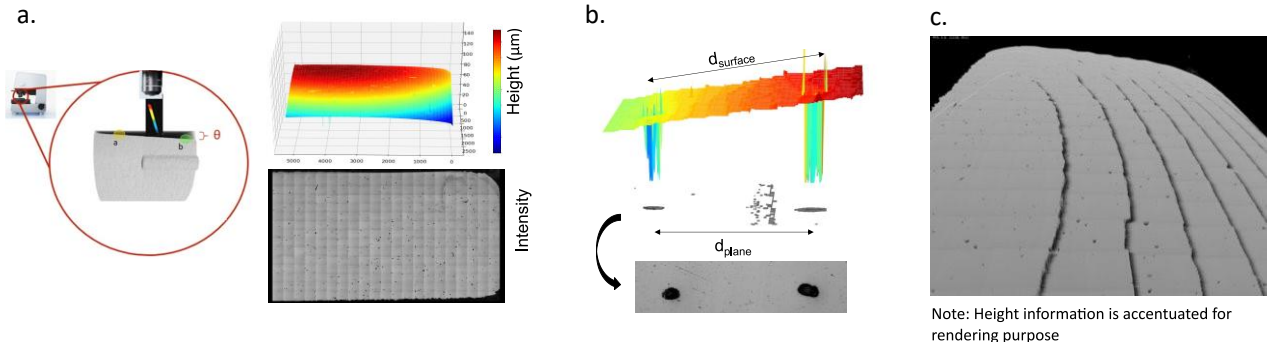

Figure 6: Laser confocal microscopy image correction: a) laser confocal imaging, b) distortion artifact from projected distance, c) corrected laser confocal microscopy image

Multimodal 2D/3D Registration

The last part of the proposed protocol consists in the final alignment of the two image modalities obtained in the previous steps, i.e. between the corrected microscopy image and the XCT slices extracted from the volume. To do so, the pores are first segmented. A global manual thresholding by an expert is performed to extract pores from the XCT volume, while the Segmentation Wizard of the Dragonfly 2021.3 (Object Research Systems, Montreal, Qc, Canada) software environment is used to apply a 3-class segmentation model (background, titanium and pores) to the microscopy image. Once the pores are identified, the marching cube algorithm is applied on the pores to convert the segmentations into meshes. Then, an alignment between the two meshes is performed using the Iterative Closest Point algorithm [5]. Once the 4x4 transformation matrix of the optimal alignment identified, this transformation is also applied to the 2.5D microscopic image in order to obtain the image-to-image correspondence.

Correlative Study

The 2D/3D registration protocol allows obtaining an optimal superposition between the microscopy image and the extracted XCT slices. Moreover, this approach enables to proceed to a pore-to-pore comparison between these two image modalities. Specifically, in this study, the variability of the morphological measurements as well as the flaw detection capabilities provided by the XCT volumes are compared with a higher resolution microscopy image used here as ground truth. To proceed, first the proposed registration protocol is applied. Then, the pores are segmented in both modalities using the same approach as describe previously. In order to make this comparison at the same resolution, the segmentations carried out in the XCT image domain are upsampled to the resolution of the microscopy images. Next, the following morphology metrics are computed for each pore: the aspect ratio, the 2D equivalent diameter and the 2D surface area. The segmentations, the morphology analysis as well as the visualization are carried out in the Dragonfly 2021.3 (Object Research Systems, Montreal, Qc, Canada) software environment.

Registration Metric

Finally, for the purpose of evaluating quantitatively the quality of the registration performed, a distance map between the isocenter coordinates of the corresponding pores identified in the two modalities is generated. In order to reduce the isocenter measurement errors affected by the uncertainty in the pore boundaries detection, the segmentations corresponding to the pores are smoothed with a 3 pixels square kernel. The distances of the dense regions (without pores) are interpolated using radial basis functions (RBF) [9].

3 Results and Discussion

In this section, results related to the quality of the multimodal 2D/3D registration will be commented first and the correlative study will be discussed next.

2D/3D Registration Evaluation

The 2D/3D multimodal registration results obtained for Samples 1, 2 and 3 are presented in Figure 7, Figure 8 and Figure 9, respectively. For each of these figures, a qualitative assessment between i) laser confocal microscopy and ii) x-ray computed tomography of the regions of interest a) and c) can be made. Furthermore, it is possible to compare the different pore segmentations obtained in each modality. It should be noted that the global thresholding segmentation of the XCT image was performed *a posteriori* to the identification of an optimal correspondence. The authors are aware that more advanced segmentation algorithms are available [13]–[15], but the evaluation of these algorithms is not the objective of the current study, but rather a subject for future comparison. Subsequently, as explained previously, these three figures present the interpolated distance map of the pore isocenter error (Figure 7b, Figure 8b and Figure 9b). This distance map allows therefore to quantify the registration fit on the entire cut surface of the sample and to realize a qualitative pore-to-pore comparison between the two modalities. By quantifying the registration deviation, we note that it corresponds to 2 pixels on average with a maximum of 8 pixels.

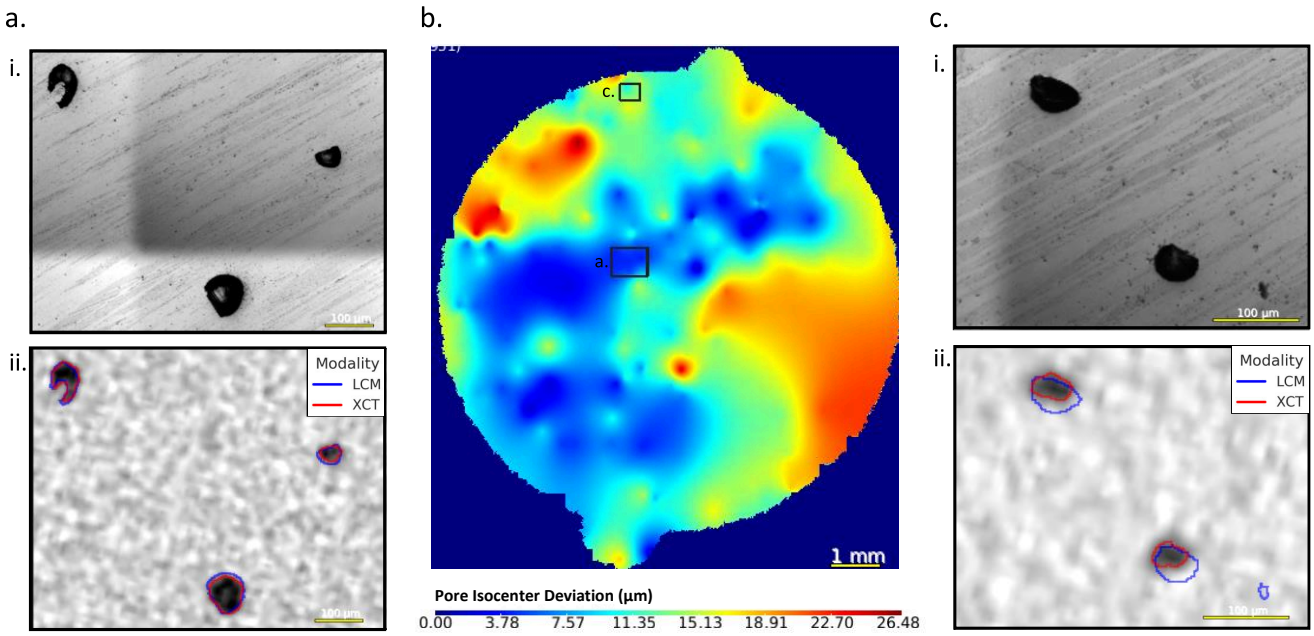

Figure 7: Registration fit between the laser confocal microscopy image (LCM) and the x-ray computed tomography volume (XCT) for Sample 1 (S1). a) i. Extracted LCM image region, ii. Corresponding XCT fit and segmentation (blue and red represent the LCM and XCT pore detections, respectively), b) Distance map between isocenters of the corresponding pores identified in the two modalities and interpolated over the complete image using the RBF interpolation, c) i. Extracted LCM image region, ii. Corresponding XCT fit and segmentation

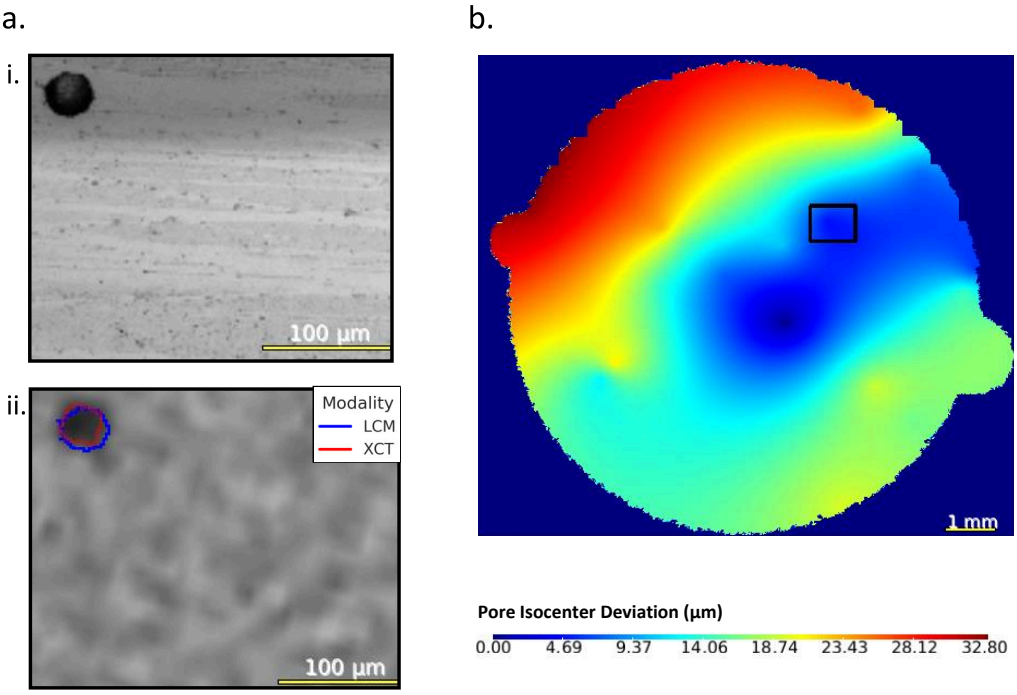

Figure 8: Registration fit between the laser confocal microscopy image (LCM) and the x-ray computed tomography volume (XCT) for Sample 2 (S2). a) i. Extracted LCM image region, ii. Corresponding XCT fit and segmentation (blue and red represent the LCM and XCT pore detections, respectively), b) Distance map between isocenters of the corresponding pores identified in the two modalities and interpolated over the complete image using the RBF interpolation

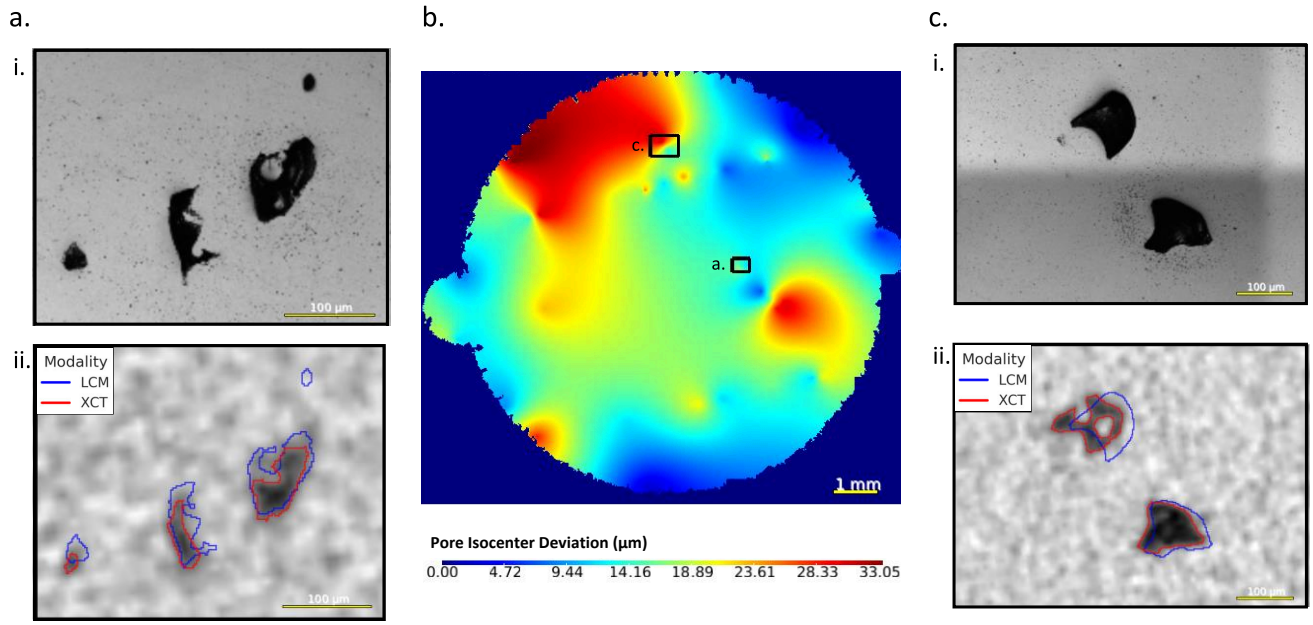

Figure 9: Registration fit between the laser confocal microscopy image (LCM) and x-ray computed tomography volume (XCT) for Sample 3 (S3). a.i). Extracted LCM image region, a.ii) Corresponding XCT fit and segmentation (blue and red represent the LCM and XCT pore detections), b) Distance map between isocenters of the corresponding pores identified in the two modalities and interpolated over the complete image using the RBF interpolation, c.i.) Extracted LCM image region, c.ii) Corresponding XCT fit and segmentation

This error sums up all the errors of the protocol: uncertainties linked to the two XCT scan acquisitions, to the rigid registration between the two volumes as well as to the 2D/3D registration. It can be noticed that the maximum registration deviation is less for Sample S1, 26.48 µm (Figure 7b) compared to Samples S2 and S3, which offer a deviation of 32.8 µm (Figure 8b) and 33.05 µm (Figure 9b), respectively. The difference to note is that Sample S1, in addition to having the highest level of porosity, presents also a random and uniform pore distribution on the surface. As the last step of the proposed registration protocol relies on the pore alignment using the ICP algorithm, the registration deviation is therefore minimized since numerous and uniformly distributed pores act as landmarks in the process. That means than the quality of registration depends on the number of pores observed and samples with no XCT visible pores would represent a limitation of our methodology. Also, the isocenter distance maps show that the registration error appears larger near the periphery of the image because of greater 2D image distortions near the image edges.

Correlative Study Results

The final porosity analysis performed on the overlapping area obtained by our proposed registration protocol are shown on Figure 10. Specifically, the 2D area (Figure 10a), the 2D equivalent diameter (Figure 10b) and the aspect ratio (Figure 10c) distributions are presented for the 3 samples. At first sight and as expected due to the difference in resolution between the two image modalities, a higher number of small pores are detected on the microscopy images. However, we observe from these graphs that from a 2D equivalent diameter higher than ~90 µm, the distributions between the two modalities tend to correspond. Contrary to Jolley et al, we do not observe a significant overestimation of the pore size measurements in the XCT image domain. Finally, we also observe from the aspect ratio distribution comparison that the pores extracted in the XCT volume tend to be more spherical, which can be explained by a lower resolution of this technique.

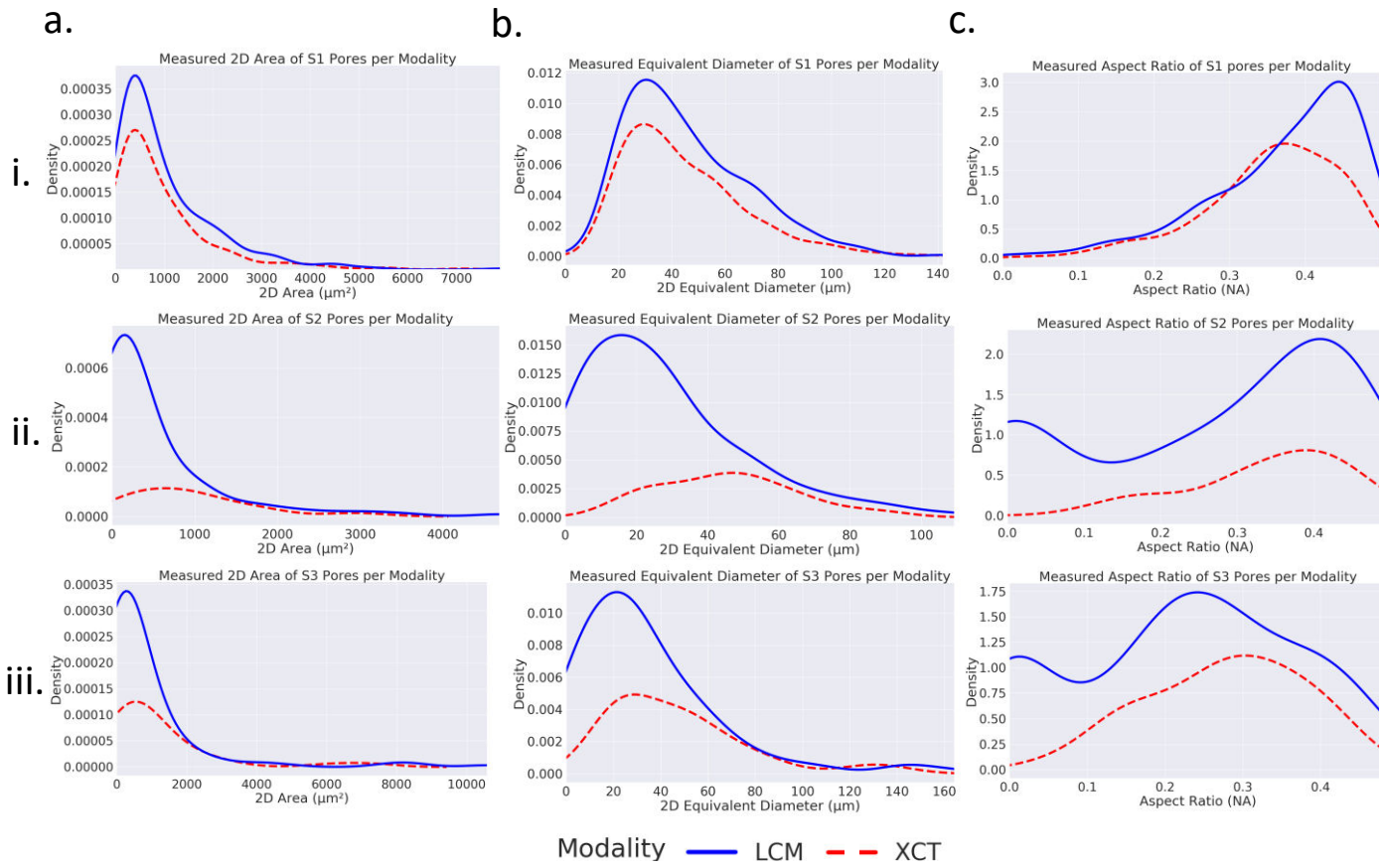

Figure 10: Porosity analysis comparison between the segmented pores in the laser confocal microscopy image (LCM) and the corresponding XCT region represented, respectively, by blue and dashed red lines. The compared morphology distribution of a) 2D area, b) 2D Equivalent Diameter and c) Aspect Ratio for i) S1, ii) S2 and iii) S3.

4 Conclusion

In this work, we propose a 2D/3D multimodal registration protocol between an x-ray computed tomography volume and a laser confocal microscopy image in order to establish a multi-scale pore-to-pore comparison. The presented results show that our methodology allows the achievement of an automated registration between the two modalities using a series of Python scripts based on the Dragonfly software and external developer tools. This approach offers the possibility to validate the XCT pore detection capability even when access to a state-of-the-art AOSS is limited. Although this registration is possible with less deviations in the center, there are still some larger deviations at the contour of the images, which will be addressed in future work. Nonetheless, this protocol allows the use of higher resolution and signal to noise ratio laser confocal microscopy images as ground truth for validation, comparison and enhancement studies related to the porosity detection in LPBF parts using X-ray computed tomography.

Acknowledgements

The authors like to express their appreciation for the financial support provided by the CRIAQ and would like to thank Etienne Moquin and Erika Judith Herrera Jimenez, PhD, for their help and expertise provided for the sample preparation and sample imaging.

References

[1] A. Thompson, I. Maskery, and R. K. Leach, “X-ray computed tomography for additive manufacturing: a review,” *Meas. Sci. Technol.*, vol. 27, no. 7, p. 072001, Jun. 2016, doi: 10.1088/0957-0233/27/7/072001.

[2] M. Seifi *et al.*, “Progress Towards Metal Additive Manufacturing Standardization to Support Qualification and Certification,” *JOM*, vol. 69, no. 3, pp. 439–455, Mar. 2017, doi: 10.1007/s11837-017-2265-2.

[3] P. Withers, J. Donoghue, and T. Burnett, “Correlative Tomography - Bridging the length-scales through correlative X-ray and Electron Imaging,” *Microscopy and Microanalysis*, vol. 27, no. S1, pp. 932–933, Aug. 2021, doi: 10.1017/S1431927621003585.
[4] T. L. Burnett *et al.*, “Correlative Tomography,” *Sci Rep*, vol. 4, no. 1, pp. 1–6, Apr. 2014, doi: 10.1038/srep04711.
[5] X. Yang, D. Gürsoy, C. Phatak, V. D. Andrade, E. B. Gulsoy, and F. D. Carlo, “Learning From Scanning Transmission Electron Microscopy to Enhance Transmission X-ray Microscopy: How We Can Merge STEM and TXM Datasets?,” *Microscopy and Microanalysis*, vol. 22, no. S3, pp. 240–241, Jul. 2016, doi: 10.1017/S1431927616002051.
[6] V. Sundar, Z. Snow, J. Keist, G. Jones, R. Reed, and E. Reutzel, “Flaw Identification in Additively Manufactured Parts Using X-ray Computed Tomography and Destructive Serial Sectioning,” *J. of Materi Eng and Perform*, vol. 30, no. 7, pp. 4958–4964, Jul. 2021, doi: 10.1007/s11665-021-05567-w.
[7] B. R. Jolley, M. D. Uchic, D. Sparkman, M. Chapman, and E. J. Schwalbach, “Application of Serial Sectioning to Evaluate the Performance of x-ray Computed Tomography for Quantitative Porosity Measurements in Additively Manufactured Metals,” *JOM*, Sep. 2021, doi: 10.1007/s11837-021-04863-z.
[8] A. A. Evans and R. E. Donahue, “Laser scanning confocal microscopy: a potential technique for the study of lithic microwear,” *Journal of Archaeological Science*, vol. 35, no. 8, pp. 2223–2230, Aug. 2008, doi: 10.1016/j.jas.2008.02.006.
[9] M. Letenneur, A. Kreitcberg, and V. Brailovski, “Optimization of Laser Powder Bed Fusion Processing Using a Combination of Melt Pool Modeling and Design of Experiment Approaches: Density Control,” *Journal of Manufacturing and Materials Processing*, vol. 3, no. 1, Art. no. 1, Mar. 2019, doi: 10.3390/jmmp3010021.
[10] P. Viola and W. M. Wells, “Alignment by maximization of mutual information,” in *Proceedings of IEEE International Conference on Computer Vision*, Jun. 1995, pp. 16–23. doi: 10.1109/ICCV.1995.466930.
[11] N. Otsu, “A Threshold Selection Method from Gray-Level Histograms,” *IEEE Transactions on Systems, Man, and Cybernetics*, vol. 9, no. 1, pp. 62–66, Jan. 1979, doi: 10.1109/TSMC.1979.4310076.
[12] W. E. Lorensen and H. E. Cline, “Marching cubes: A high resolution 3D surface construction algorithm,” *Computer Graphics*, vol. 21, no. 4, pp. 163–169, 1987.
[13] J. Lifton and T. Liu, “An adaptive thresholding algorithm for porosity measurement of additively manufactured metal test samples via X-ray computed tomography,” *Additive Manufacturing*, vol. 39, p. 101899, Mar. 2021, doi: 10.1016/j.addma.2021.101899.
[14] V. A. J. Jaques *et al.*, “Review of porosity uncertainty estimation methods in computed tomography dataset,” *Meas. Sci. Technol.*, vol. 32, no. 12, p. 122001, Aug. 2021, doi: 10.1088/1361-6501/ac1b40.
[15] C. Gobert, A. Kudzal, J. Sietins, C. Mock, J. Sun, and B. McWilliams, “Porosity segmentation in X-ray computed tomography scans of metal additively manufactured specimens with machine learning,” *Additive Manufacturing*, vol. 36, p. 101460, Dec. 2020, doi: 10.1016/j.addma.2020.101460.